CMS Physics Analysis Summary

Contact: cms-pag-conveners-exotica@cern.ch 2016/08/04

Search for displaced leptons in the e-mu channel

The CMS Collaboration

Abstract

A search for new long-lived particles decaying to electrons and muons is presented using data from proton-proton collisions produced in 2015 by the LHC at $\sqrt{s} = 13\,\text{TeV}$. Data used for the analysis were collected by the CMS detector and correspond to an integrated luminosity of $2.6\,\text{fb}^{-1}$. Events are selected with an electron and muon that both have transverse impact parameter values between $200\,\mu\text{m}$ and 10 cm. Since no significant excess is observed, limits are set on the Displaced Supersymmetry model, with pair production of top squarks decaying into an e-mu final state via R-parity-violating interactions. The results are the most restrictive to date on this model. For a top squark mean proper decay length of 2 cm, masses below 870 GeV are excluded at 95% confidence level.

1 Introduction and theoretical motivation

Naturalness dictates that new physics should appear at the TeV scale to explain the observed value of the Higgs mass at the electroweak scale. To date, the experiments at the CERN LHC have not observed any physics beyond the standard model (BSM). The vast majority of BSM searches assume that any new particles produced will decay promptly. Since these searches are optimized for promptly decaying particles, their sensitivity to signatures involving long-lived BSM particles is greatly reduced. Therefore, new physics at the LHC containing displaced decays is relatively less constrained although both the CMS and ATLAS Collaborations have performed dedicated searches for decays of BSM particles with long lifetimes. Direct search strategies include finding BSM particles via anomalous energy loss and/or low velocity [1, 2] or via a disappearing track signature [3, 4]. There are also numerous indirect searches targeting the decay products of long-lived particles. They target non-prompt final-state jets [5], photons [6–8], leptons [9, 10], or combinations thereof [11].

A recent CMS search in the displaced e-μ final state [10] was optimized to BSM particle lifetimes longer than the sensitive regime of prompt searches but shorter than the optimal lifetimes for other searches for long-lived BSM signatures. It also dispensed with the requirement that the displaced final state particles originate from a common vertex. This summary describes an improved version of that previous search using data collected in 2015 at $\sqrt{s} = 13\,\text{TeV}$. It employs an improved trigger strategy and a new data-driven QCD background estimation method. As before, the search is designed to be generic in order to be sensitive to as much of the open model space as possible. Consequently, the event selection focuses exclusively on a displaced, isolated lepton signature and does not try to identify signal events using hadronic activity or missing energy. In this way, we retain sensitivity to any model that can produce leptons with displacements on the order of 100 μm to 10 cm, regardless of whether these leptons are accompanied by jets, missing transverse energy ($\not\!\!E_T$), or other interesting features.

We interpret the search results in the context of the Displaced Supersymmetry [12] model. This model introduces R-parity violating terms in the superpotential of the minimally supersymmetric standard model. R-parity violation (RPV) allows the lightest supersymmetric particle (LSP) to decay into SM particles. This can frustrate standard SUSY searches by lessening or removing the missing energy signature generally present in SUSY topologies. Only lepton number-violating operators are considered to avoid constraints from proton decay. With sufficiently small couplings for these operators, the LSP will have a long enough lifetime that its decay products are measurably displaced from the region of beam-beam overlap in which the proton-proton interactions occur (henceforth referred to as the "luminous region"). For a large range of these couplings, Displaced Supersymmetry can generate a natural SUSY model that could have easily escaped detection thus far at the LHC.

We focus on the case in which the LSP is the top squark, the superpartner of the top quark. At the LHC, top squarks would be dominantly produced in pairs. The top squarks in our benchmark model then decay through an RPV vertex, $\widetilde{\text{t}}_1 \to \text{bl}$, where l is an electron, muon, or tau lepton. For simplicity, we assume lepton universality in the top squark decay vertex, so that the branching fraction to any lepton flavor is equal to one third. We conduct a search for decays of top squark pairs in which there is an electron and a muon in the final state, with both of the leptons being displaced from the luminous region.

2 Data and Monte Carlo simulation samples

This analysis uses pp collision data taken in 2015 at $\sqrt{s} = 13$ TeV, corresponding to an integrated luminosity of 2.6 ± 0.1 fb^{-1}. The events in the search sample are collected by a dedicated trigger that targets displaced e-μ pairs. It requires a muon with momentum perpendicular to the beam axis, p_{T}, above 38 GeV. To target displaced electrons, the trigger requires a cluster in the electromagnetic calorimeter with the transverse energy above 38 GeV. To increase the acceptance for displaced muons, no cuts on the impact parameter or matching to a primary vertex are required for the muon leg of the trigger. To increase acceptance for displaced electrons, no tracking information is used in the electron leg of the trigger.

In order to evaluate contributions from SM background and potential signal processes, samples are produced via Monte Carlo (MC) simulation techniques. SM background samples are simulated using PYTHIA 8 [13] with MADGRAPH, or using POWHEG. All background estimates are derived from the simulation with the exception of heavy flavor QCD processes (HF). Given the large HF cross-sections at the LHC, we develop a data-driven estimate for these processes.

Samples of the process pp$\rightarrow\widetilde{\mathrm{t}}_1\widetilde{\mathrm{t}}_1^*$, with the top squarks decaying via $\widetilde{\mathrm{t}}_1\rightarrow$bl, were generated using PYTHIA 8. Starting with a SUSY Les Houches Accord (SLHA) file [14] corresponding to Snowmass Points and Slopes (SPS) point 1a [15], the mass and width of the top squark were modified to produce samples corresponding to different points in model parameter space. Specifically, samples are generated with top squark masses between 200 and 1200 GeV and lifetimes over a range of 0.1 to 100 cm/c.

3 Event selection

The event selection can be grouped into two stages. First, we select events with exactly one electron and one muon that are well-reconstructed and isolated. The leptons are required to be oppositely charged. This stage will subsequently be referred to as the analysis "preselection". The second stage involves classifying the events passing the preselection based on the offset of the selected leptons' trajectories from the beam axis in the transverse plane of the detector.

3.1 Preselection

The preselection requirements aim at selecting events which contain exactly two well identified leptons in the final state, specifically one electron and one muon. The leptons are reconstructed using the particle-flow event reconstruction algorithm [16], which combines information from all the CMS sub-detectors in order to reconstruct all stable particles and determine their types, directions and energies.

Muon candidates are built using a combination of the track parameters measured in the inner tracker and the muon system [17]. A set of muon identification criteria are applied to select well-reconstructed muons with good track qualities in both the inner tracker and the muon systems. Muon isolation is enforced using a particle-flow based method. The discriminant is defined as the scalar sum of the transverse momenta of all particles, excluding the muon, within a cone of $\Delta R \equiv \sqrt{(\Delta\eta)^2 + (\Delta\phi)^2} < 0.4$ around the muon, where η is pseudorapidity and ϕ is the azimuthal angle in the plane transverse to the beam axis. Charged hadrons from additional p-p interactions (pileup) are not considered in the isolation sum. The contribution from pileup interactions to the neutral component of the isolation is additionally corrected using the $\Delta\beta$ method on an event-by-event basis [18]. The isolation of the muon is required to be less than 15% of the muon's p_{T}.

Electron candidates are reconstructed by combining information from deposits in the electromagnetic calorimeter (ECAL) and tracks built by the Gaussian sum filter algorithm [19]. A set of electron identification criteria are applied to select electrons with compatible signatures in the tracker and ECAL. Electron candidates that traverse the overlap region between the barrel and endcap detectors are rejected because of the reduced reconstruction performance in this region. Similar to the muon case, electron isolation is achieved using a particle-flow based method but with a cone size of $\Delta R < 0.3$ around the electron. The contribution from neutral hadrons from additional p-p interactions is accounted for using the FastJet [20] energy density (ρ) in the event. The isolation sum is required to be less than 3.5% (6.5%) of the electron's p_{T} for electrons in the barrel (endcap) region.

To remain within the region of detector acceptance, leptons are required to have absolute pseudorapidity less than 2.4. To ensure we are operating well above the momentum thresholds required at the trigger level, we require the electrons (muons) in the event to have a transverse momentum greater than 42 GeV (40 GeV).

Each event is required to have exactly one electron and one muon passing all the criteria discussed above. In these events, the two leptons are required to be oppositely charged and separated by $\Delta R > 0.5$.

The events passing the preselection are further categorized using the track impact parameter of the selected leptons in the plane transverse to the proton beams. This transverse impact parameter ($|d_0|$) is defined as the distance of closest approach in the transverse plane of the helical trajectory of the lepton track to the beam axis. The lepton's impact parameter is strongly correlated with the lifetime of its parent particle. This feature is exploited to construct both control regions used for background estimation and validation as well as search regions with high signal efficiency and very little background contamination. These regions are detailed in the following sections and summarized in Table 1.

3.2 Background control regions

The "prompt control region" contains all events passing the preselection in which both leptons meet the extra requirement of $|d_0| < 100\,\mu$m. This region is dominated by standard model processes with prompt leptons and is used to check that the MC simulation accurately reproduces the behavior of the data. The "displaced control region" requires instead that both leptons have $100 < |d_0| < 200\,\mu$m. This region is enriched in background processes with genuinely displaced leptons and is used for the data-driven QCD estimation as described in Section 5.2.3.

3.3 Signal search regions

By requiring both the electron and the muon in the events passing the preselection to have large enough impact parameters, we can construct a region that is largely free of leptons from SM processes. The efficiency for a lepton to pass a given d_0 cut is highly correlated with the lifetime of its parent particle. Consequently, a given d_0 cut will have drastically different efficiencies at different values of the parent particle lifetime. As a result, we define three search regions and use them simultaneously to probe a wide range of lifetimes. The tight search region (SR III), requiring $|d_0| > 1000\,\mu$m for both leptons, is expected to have very low background contamination. Events enter the intermediate search region (SR II) if they fail the cuts defining the tight region but both leptons have $|d_0| > 500\,\mu$m. Similarly, events enter the loose search region (SR I) if they fail to enter the intermediate one but both leptons have $|d_0| > 200\,\mu$m. This loose search region is expected to contain more background contamination, but retain higher signal efficiency for the shorter top squark lifetimes. These regions are constructed such that

there is no overlap between them so that they can be used in combination when calculating upper limits on signal contribution. An upper limit of 10 cm is placed on the lepton impact parameters. This ensures that the leptons originate within the pixel tracker, since the lepton identification criteria require hits in at least one pixel layer. Table 1 summarizes the control and search regions defined by specific lepton impact parameter criteria. Figure 1 shows the areas of the lepton impact parameter parameter space defined by the different control and search regions.

Table 1: Names, purposes, and selection criteria of regions based on $|d_0|$ ranges. Preselection criteria are applied to all listed regions.

Region	Purpose	Selection Criteria
Prompt Control Region (CR I)	Validation of MC Simulation	$\|d_0\|_{e,\mu} < 100\,\mu$m
Displaced Control Region (CR II)	Data-driven HF Estimation	$100 < \|d_0\|_{e,\mu} < 200\,\mu$m
Displaced Electron Region (CR III)	Validation of HF Estimation	$\|d_0\|_e > 100\,\mu$m $\|d_0\|_\mu < 200\,\mu$m
Displaced Muon Region (CR IV)	Validation of HF Estimation	$\|d_0\|_\mu > 100\,\mu$m $\|d_0\|_e < 200\,\mu$m
Search Region I (SR I)	Loose Search Region	$\|d_0\|_{e,\mu} > 200\,\mu$m not in SR II
Search Region II (SR II)	Medium Search Region	$\|d_0\|_{e,\mu} > 500\,\mu$m not in SR III
Search Region III (SR III)	Tight Search Region	$\|d_0\|_{e,\mu} > 1000\,\mu$m

4 Corrections to MC simulation

In order to account for known differences between the MC simulation and data, various corrections are applied to the MC simulation. Detailed descriptions of the major sources of these differences and the methods used to correct them are given in the following sections.

4.1 Corrections to leptons

Scale factors are produced by CMS to account for possible differences in the reconstruction and identification performance of the leptons in data and simulation. Even though these scale factors are produced using prompt leptons, they are still valid for our use case since most of the leptons needing to be corrected are prompt. To account for the differences in reconstruction efficiency in data and simulation for leptons with larger impact parameters, Section 6 conveys a dedicated study to assess the systematic uncertainties.

The scale factors are calculated using a tag and probe method, which takes advantage of the fact that the dilepton invariant mass in Z→ll decays has a very narrow peak centered at M_Z. The resonances are often reconstructed as pairs so that by requiring one leg to pass a tight identification (tag) and one to pass a loose identification (probe) one can perform a study using the probes without a bias brought by the selections. The corrections obtained are generally of the order of 5% and do not have a large effect on the results of this search.

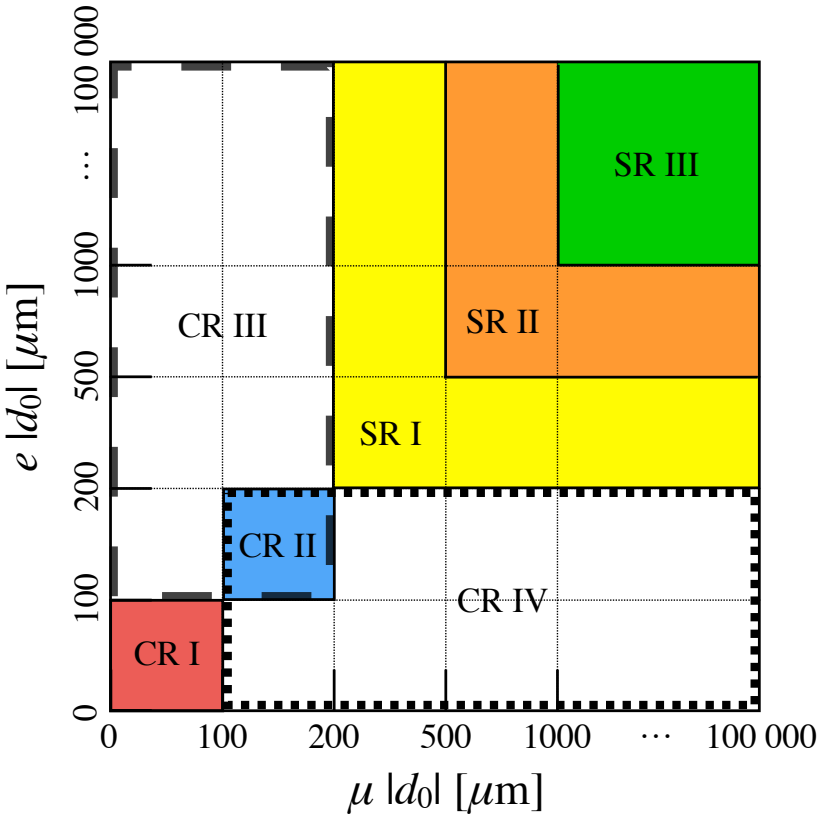

Figure 1: Diagram of control and search regions based on lepton impact parameter. CR I corresponds to the prompt control region, CR II corresponds to the displaced control region, and CR III (IV) corresponds to the region with a displaced electron (muon). Note that CR II is a subset of both CR III and CR IV. SR I, SR II, and SR III correspond to the three search regions.

4.2 Trigger efficiency corrections

The trigger efficiency is calculated using an orthogonal data set collected using jet and $\not{E}_T$ triggers in order to remove any potential bias from using triggers related to electrons or muons. We choose to enrich the data sample in fully leptonic $t\bar{t}$ events as this is the largest source of e-μ events in the kinematic regime of interest. We apply the analysis preselection (as described in section 3.1) with extra cuts requiring two jets with $p_T > 30$ GeV, $|\eta| < 2.4$ and at least one passing the medium CSV b-tag working point (>0.8).

The trigger scale factor is defined as an efficiency after applying the preselections plus the $t\bar{t}$-enriching selections above. The numerator is the number of events in data passing the jet/$\not{E}_T$ triggers that also pass the signal trigger over the total number of events which pass the jet/$\not{E}_T$ trigger. The denominator is calculated in a similar way using the simulated $t\bar{t}$ sample. The final scale factor applied to the yields from MC simulation is 0.975 ± 0.009.

5 Background Estimation

At the LHC, the vast majority of leptons from SM processes come from promptly-decaying particles. However, displaced leptons can arise from decays of τ leptons and B or D mesons ($c\tau_\tau \approx 87\,\mu$m, $c\tau_B \approx 500\,\mu$m, $c\tau_D <\approx 100\,\mu$m). MC simulation of all of the relevant SM processes have large effective luminosities and are well modeled with the exception of heavy flavor QCD. As a result we use MC simulation to estimate the contributions from $Z\to\tau\tau$, $t\bar{t}$, diboson and single top processes while employing a data-driven method to estimate the contribution from HF.

5.1 Estimation of contribution from non-QCD events

Due to the limited size of the SM background MC samples, directly counting small number of events expected in the search regions yields very large statistical uncertainties. Instead, we produce a parametrization using the following technique. We factorize the electron and muon requirements, weighting the yield for each sample after the preselection by the efficiency for each lepton leg to pass a given impact parameter requirement. In other words, instead of simultaneously applying $|d_0|$ cuts on both leptons and counting the remaining events, we apply the $|d_0|$ cut for a given search region separately on each lepton, calculating the efficiency for each lepton, and then multiply the initial number of events in the sample by the product of the electron efficiency and muon efficiency to produce the estimate in the given search region. If the efficiency for either lepton to pass the $|d_0|$ requirement drops to zero, the cut is loosened until a non-zero efficiency can be calculated. This yields a conservative upper limit on the contribution from the sample in question. A closure test has been performed over a range of $|d_0|$ requirements to verify that the yields obtained by direct counting agreed with those obtained by applying the parametrization method.

5.2 Estimation of contribution from heavy flavor QCD events

To estimate the contribution from HF processes in the search regions, we scale the estimation in the displaced control region ($100 < |d_0|_{e,\mu} < 200\,\mu$m) using scale factors derived in HF-enriched control regions in data. We use the lepton impact parameter spectra in these control regions to derive the scale factors. The following sections detail the definitions of the control regions, the studies performed to validate these regions, and the calculation and implementation of the scale factors.

5.2.1 Heavy flavor + lepton control regions

We construct control samples in data dominated by pair production of heavy flavor quarks in which the decay chain of one of the quarks contains a lepton. We leverage the properties of HF dijet events to use a tag and probe methodology in which the tag jet is required to pass one of the working points of the combined secondary vertex b-tagging algorithm (CSV) used at CMS [21] and the probe jet is required to have a reconstructed lepton nearby ($|\Delta R| < 0.5$). The probe jet is not subjected to the CSV requirement since track impact parameter is one of the variables included in the CSV discriminant and choosing jets with high CSV value will tend to select leptons with higher $|d_0|$ values, biasing the $|d_0|$ distribution. To reduce contamination from $t\bar{t}$, we make two additional selections. First, we require the tag and probe jets to be back-to-back in the transverse plane ($|\Delta\phi| > 2.5$). Secondly, we require the lepton in the event to have $|d_0| > 100$ μm. Separate control regions are defined for electrons (HF+e) and muons (HF+μ), collected using a single electron trigger and a single muon plus jet trigger, respectively. The trigger for the HF+μ region was prescaled during 2015 data-taking and only collected 28.7 pb^{-1}. Figure 2 shows the lepton $|d_0|$ in these control regions. These regions represent pure samples of HF events, with small contaminations from non-HF backgrounds predominantly having small impact parameter values and decreasing rapidly with increasing $|d_0|$. Due to the limited number of events in the simulation of HF processes with electrons, the tail of the $|d_0|$ distribution is not properly populated. This effect is not included in the statistical uncertainties displayed in each bin. In the muon case, the simulation represents a much larger number of events and this effect is not seen. This limitation of the HF simulation is the primary motivation for the data-driven estimation technique we employ.

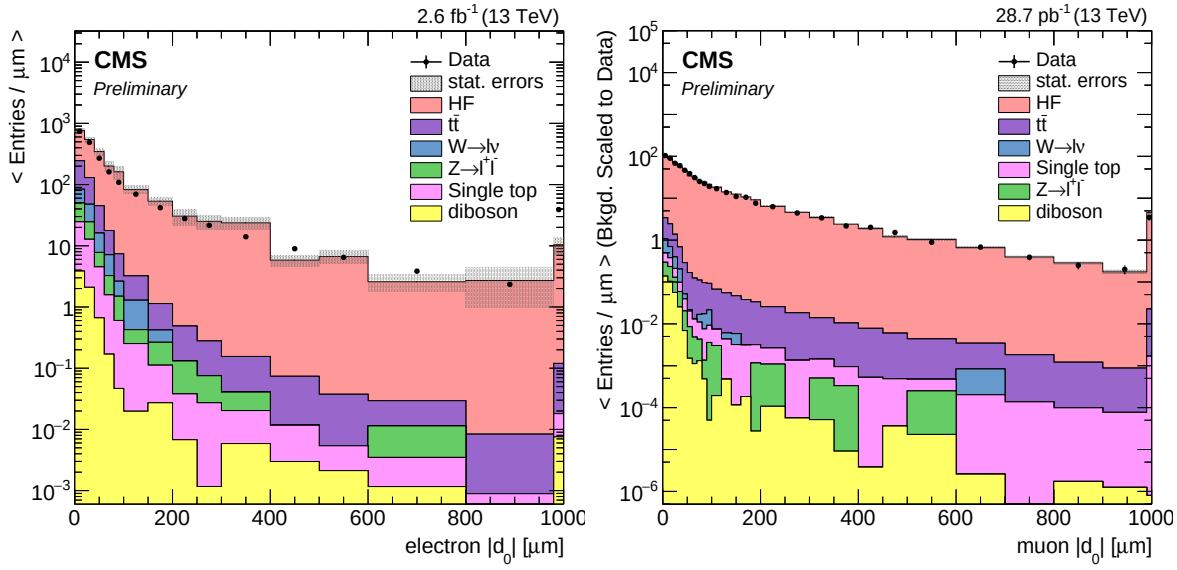

Figure 2: Lepton $|d_0|$ spectra in the HF+e (left) and HF+μ (right) control regions with corresponding dedicated lepton-flavor-specific HF simulation used in each case. The rightmost bin of each plot contains the overflow entries.

5.2.2 HF + lepton control region validation

As will be detailed in section 5.2.3, we use the lepton $|d_0|$ spectra from the HF + lepton control regions to model the background from HF in our search regions. We must therefore validate that the spectra obtained are valid proxies for the spectra in the target region. A direct comparison between data in the control and search region is ill-advised due to the potential presence of

signal events in the search region. We instead add a requirement that the isolation variable be between 0.15 and 1.5 for events in both the HF + lepton control regions and the preselection (as described in section 3.1) and compare the lepton $|d_0|$ spectra in these HF-enriched regions with non-isolated leptons. We prefer to avoid observing the subset of the anti-isolated preselection region in which both leptons are displaced, since this space could potentially be populated by new physics. Therefore, when obtaining the $|d_0|$ spectrum for one lepton flavor we require the other lepton in the event to be prompt ($|d_0| < 200$ μm). Figure 3 shows that the spectra in these different regions are indeed compatible and gives confidence that the leptons in the HF + lepton control regions are a good model for the leptons from HF in the signal regions.

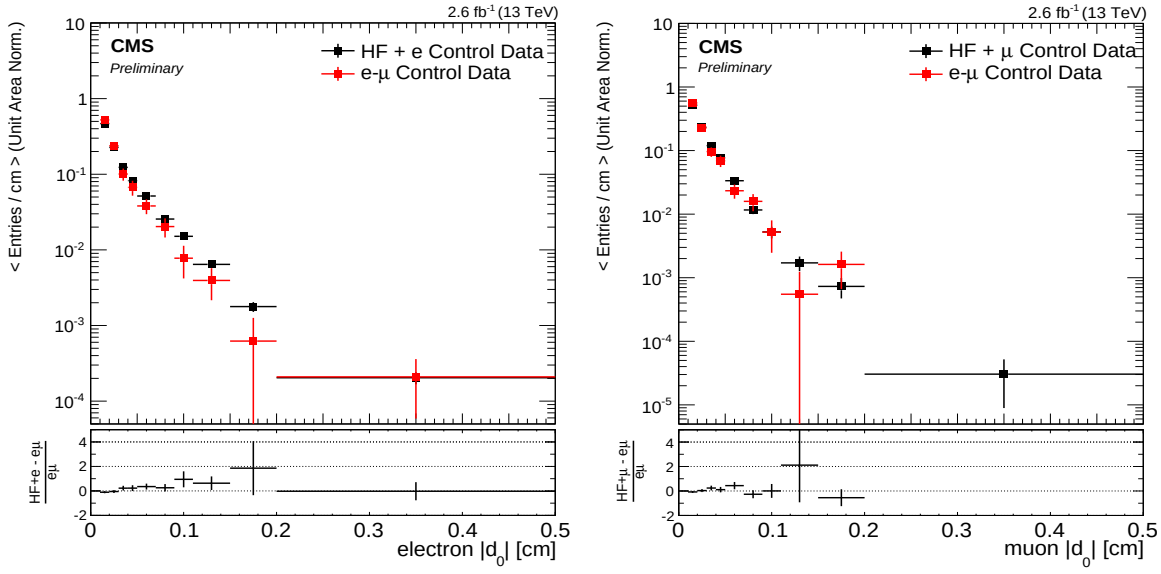

Figure 3: Lepton $|d_0|$ spectra in the HF + lepton (black) and anti-isolated preselection (red) regions for electrons (left) and muons (right). Event yields per bin have been divided by the bin width. The rightmost bin of each plot contains the overflow entries. The lower frame shows the difference between the HF+l control data and the e-μ control data, normalized to the e-μ control data.

We finally prepare the lepton $|d_0|$ spectra for use in the final background estimations by making two additional modifications. First, in order to avoid any bias due to correlations between lepton isolation and $|d_0|$, we apply the same lepton isolation requirements as in the preselection to the leptons in the HF + lepton regions. Secondly, we subtract the small residual contribution from other SM processes in this HF + isolated lepton region as predicted by the SM MC samples. The final spectra are then used to derive scale factors as described in the following section.

5.2.3 HF background estimation methodology

The estimate of HF events in the search regions is obtained by scaling the number of expected HF events in a control region using scale factors obtained from the spectra prepared from the HF + lepton control regions as described in the previous section. The HF yield to be scaled is obtained in the displaced control region. As Table 2 shows, this region is populated by one event in the 2015 data set used in this search. However, one can not draw the conclusion that HF is negligible given the large statistical uncertainty in the data yield. We apply a Bayesian approach, using a flat prior for the HF contribution and assuming the non-HF MC sum follows

a Gaussian distribution. We estimate the 68% confidence level upper limit on the HF contribution in this region to be 1.7 events.

Table 2: Yields in the displaced control region. Background and signal expectations are quoted as $N_{exp} \pm 1\sigma$ (stat) $\pm 1\sigma$ (syst).

Event Source	$100 < \lvert d_0 \rvert < 200\,\mu$m
W$\to$lν	$0.005 \pm 0.002 \pm 0.001$
single top	$0.046 \pm 0.006 \pm 0.003$
diboson	$0.083 \pm 0.018 \pm 0.004$
Z$\to$ll	$0.55 \pm 0.10 \pm 0.03$
$t\bar{t}$	$0.43 \pm 0.01 \pm 0.03$
non-QCD background sum	$1.11 \pm 0.10 \pm 0.04$
observation	1

The HF expectation in the displaced control region is then scaled to produce the HF expectation in each of the three search regions. In the HF + lepton control regions, we count the events populating two regions of the $|d_0|$ spectrum. First, we count events with lepton impact parameter values consistent with our displaced control region (N_{CR}). Secondly, we count events with lepton impact parameter values consistent with each of our search regions (N_{SR}). For a given search region, a lepton scale factor can be calculated as $\kappa_l = N_{SR}/N_{CR}$, where l is a given lepton flavor. The overall event scale factor is then the product of the electron and muon scale factors: $\kappa_{event} = \kappa_e\,\kappa_\mu$. The event scale factors are calculated to be 1.7 ± 0.35 (SR I), 0.28 ± 0.07 (SR II), and 0.011 ± 0.006 (SR III). Multiplying the upper limit on the HF contribution to the displaced control region (1.7 events) by these scale factors, the upper limits on the HF contribution in the three search regions are calculated to be 3.0 (SR I), 0.50 (SR II), and 0.019 (SR III).

This method is validated with a closure test performed using sideband regions with anti-isolated leptons. We employ the estimation method described above using anti-isolated leptons in the HF+l control regions. We derive scale factors to obtain the yields in the displaced electron (CR III) and displaced muon (CR IV) control regions with anti-isolated leptons. The estimations achieved by directly counting the number of events agree well with those by applying the method described above.

6 Systematic Uncertainties

There are several sources of systematic uncertainty considered in this analysis. For those that are common to all CMS searches, such as systematic uncertainties due to pileup, luminosity, lepton corrections, PDFs, cross-sections and trigger efficiency, we assess them using well established methods used by CMS. In what follows, we detail the dedicated methods for systematic uncertainties more specific to this analysis such as the uncertainties from the data-driven HF background estimation and the efficiency of finding displaced tracks.

The systematic uncertainty introduced by the data-driven HF background estimation is the dominant systematic effect in this search. To assess this systematic uncertainty, we vary the requirement on the b-tagging discriminant over the full range of possible values on the probe jet near the leptons in the HF + isolated lepton control regions and take the largest relative deviation seen in the scale factor as the systematic uncertainty. The same procedure is performed for

each scale factor individually and the systematic uncertainties are 32%, 80% and 92% in search region I, II and III, respectively.

The uncertainties due to the modeling of pileup events in the MC simulation is estimated by varying the cross-section of minimum bias events by 5% up and down when generating the target pileup distributions. The pileup reweighting factors calculated using these three target distributions are then applied to the preselections to obtain the variation in yields, which is taken as the systematic uncertainly on the procedure. To find the systematic uncertainty associated with the corrections to the leptons, we fluctuate the lepton scale factors up and down by their uncertainty and observe the change in the event yields. The larger deviation is taken as the uncertainty of a given sample.

To study the performance of reconstructing tracks with large impact parameters, we use a sample of cosmic muon events. These events were collected using dedicated triggers during downtime in the LHC collision scheme. We take advantage of the fact that both the muon chambers and the silicon tracker are used in the muon reconstruction. The tracking efficiency is determined by measuring the fraction of cosmic rays that are associated within an azimuthal angle of 0.2 with a track reconstructed in the tracker. Only tracks of $p_{\mathrm{T}} > 15\,\mathrm{GeV}$ are considered. In addition, tracks are required to have at least one pixel hit to mirror the lepton track selection used in this search. The uncertainty is found to be 12% in the efficiency to reconstruct both dilepton tracks. This uncertainty is applied to all expected yields from signal simulation.

Table 3 summarizes the uncertainties considered for all processes for which Monte Carlo simulation is used.

Table 3: Sources of systematic uncertainty on simulation-based estimates in this search, in percent. The rightmost column includes all the relevant systematic uncertainties, not only those explicitly mentioned in the table. For simulated signal processes, the minimum and maximum uncertainty for any value of top squark mass and lifetime are shown.

Dataset	Cross-section	Pileup	e ID/ISO	μ ID/ISO	Total
$W\to l\nu$	3.8	10.2	1.9	0.29	11.1
single top	4.2	0.2	2.9	0.22	5.1
diboson	2.5	0.2	2.9	0.23	3.8
$Z\to ll$	3.8	1.1	2.5	0.18	4.7
$t\bar{t}$	6.1	0.9	2.9	0.22	6.8
signal	$13-18$	$0.2-8.9$	$3.0-4.4$	$0.25-0.32$	$18-24$

7 Results

Table 4 shows the expected and observed numbers of events in the three search regions. In all three search regions, the HF background is the dominant expected contribution, as the expected yield from non-HF processes is much less than one event. The full selection efficiency for signal events with a final-state electron and muon varies between 0 and 15%. The selection efficiency increases with top squark mass and is maximal for a mean proper decay length of 2 cm. Since we do not observe any significant excess over the background expectation, we set 95% CL upper limits on the cross section for top squark pair production at 13 TeV. We perform this as a simultaneous counting experiment in three bins corresponding to the three search regions. We use a Bayesian calculation assuming a flat prior for the signal as a function

of top squark mass. Nuisance parameters arising from statistical uncertainties are modeled as gamma distributions, while all others are modeled as log-normal distributions. These cross section limits are translated into upper limits on the top squark mass, where the cross section for each mass hypothesis is calculated at next-to-leading-order and next-to-leading-logarithmic precision within a simplified model with decoupled squarks and gluinos [22–24]. The resulting expected and observed limit contours are shown in Figure 4 with the region to the left of the contours being excluded. We are able to exclude top squark masses up to 870 GeV for a mean proper decay length of 2 cm, setting a stronger limit on the displaced supersymmetry benchmark model than the analogous 8 TeV search, which excludes top squark masses up to 790 GeV for the same lifetime.

Table 4: Numbers of expected and observed events in the three search regions. Systematic and statistical uncertainties are added quadratically and the sum is quoted.

Event Source	Search Region I	Search Region II	Search Region III
$W\to l\nu$	$(1.1 \pm 0.5) \times 10^{-3}$	$(2.4 \pm 1.7) \times 10^{-5}$	$(0.25 \pm 0.29) \times 10^{-5}$
single top	$(8.4 \pm 1.2) \times 10^{-3}$	$(35 \pm 12) \times 10^{-5}$	$(1.50 \pm 0.91) \times 10^{-5}$
diboson	$(18.2 \pm 5.8) \times 10^{-3}$	$(39 \pm 25) \times 10^{-5}$	$(4.0 \pm 4.6) \times 10^{-5}$
$Z\to ll$	$(115 \pm 25) \times 10^{-3}$	$(100 \pm 160) \times 10^{-5}$	$(69 \pm 71) \times 10^{-5}$
$t\bar{t}$	$(60.6 \pm 5.1) \times 10^{-3}$	$(226 \pm 25) \times 10^{-5}$	$(8.0 \pm 1.6) \times 10^{-5}$
non-HF sum	$(203 \pm 26) \times 10^{-3}$	$(410 \pm 170) \times 10^{-5}$	$(82 \pm 71) \times 10^{-5}$
data-driven HF	< 3.0	< 0.50	< 0.019
total background	< 3.2	< 0.50	< 0.020
observation	1	0	0
$pp\to\tilde{t}_1\tilde{t}_1^*(M_{\tilde{t}_1} = 700\,\text{GeV})$			
$c\tau = 0.1\,\text{cm}$	3.8 ± 0.2	0.94 ± 0.06	0.16 ± 0.02
$c\tau = 1\,\text{cm}$	5.2 ± 0.4	4.1 ± 0.3	7.0 ± 0.3
$c\tau = 10\,\text{cm}$	0.8 ± 0.1	1.0 ± 0.1	5.8 ± 0.2
$c\tau = 100\,\text{cm}$	0.009 ± 0.005	0.03 ± 0.01	0.27 ± 0.03

8 Summary

A search has been performed for new physics with an electron and muon in the final state which are displaced transversely from the LHC luminous region, with no requirements made on jets or missing energy. The data sample corresponds to $2.6\,\text{fb}^{-1}$ of proton-proton collisions recorded by the CMS detector at the LHC during the 2015 run at $\sqrt{s} = 13\,\text{TeV}$. No excess is observed above the estimated number of background events for displacements up to 10 cm. The results are interpreted in the context of the displaced supersymmetry model with a top squark LSP having a lifetime up to $100\,\text{cm}/c$. We place limits at 95% CL on this model as a function of top squark mass and top squark lifetime. For a lifetime hypothesis of $2\,\text{cm}/c$, we exclude top squarks up to 870 GeV in mass.

References

[1] CMS Collaboration, "Searches for Long-lived Charged Particles in Proton-Proton Collisions at $\sqrt{s} = 13$ TeV", Technical Report CMS-PAS-EXO-15-010, CERN, Geneva,

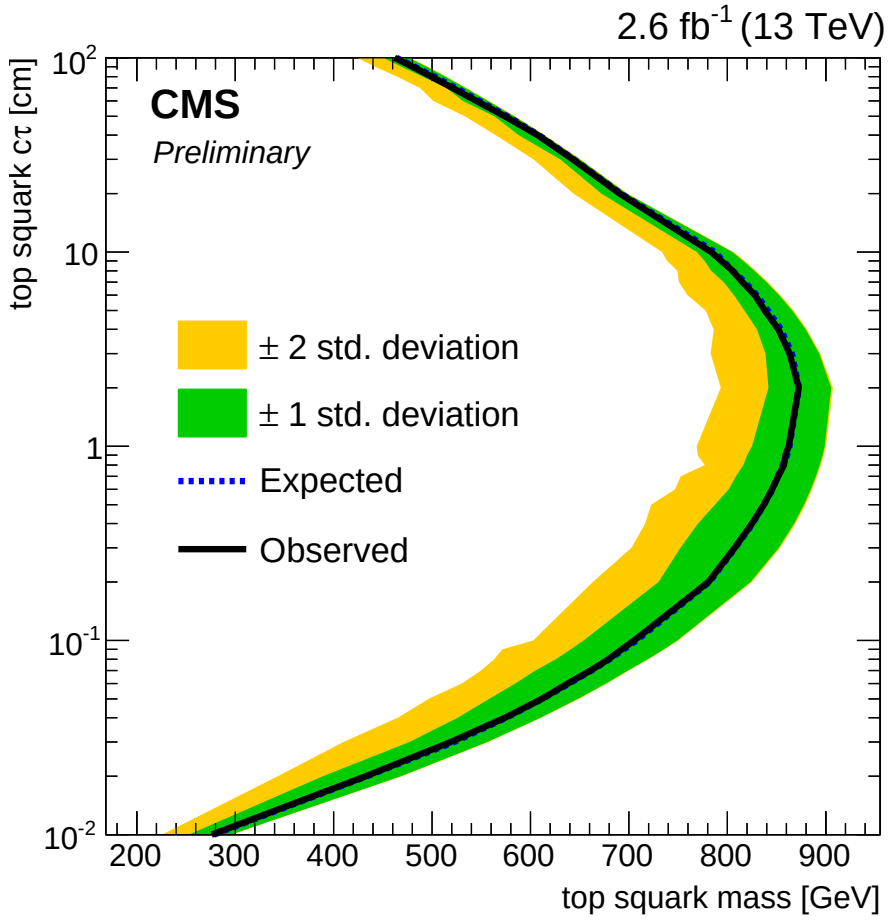

Figure 4: Expected and observed 95% exclusion contours for top squark pair production in the plane of top squark $c\tau$ and mass. The region to the left of the contours is excluded by this search.

2015.

[2] ATLAS Collaboration, "Searches for heavy long-lived charged particles with the ATLAS detector in proton-proton collisions at $\sqrt{s} = 8$ TeV", *Journal of High Energy Physics* **2015** (2015), no. 1, 1–51, doi:10.1007/JHEP01(2015)068.

[3] CMS Collaboration, "Search for disappearing tracks in proton-proton collisions at $\sqrt{s} = 8$ TeV", *JHEP* **01** (2015) 096, doi:10.1007/JHEP01(2015)096, arXiv:1411.6006.

[4] ATLAS Collaboration, "Search for charginos nearly mass degenerate with the lightest neutralino based on a disappearing-track signature in pp collisions at $\sqrt{(s)}$=8 TeV with the ATLAS detector", *Phys. Rev. D* **88** (Dec, 2013) 112006, doi:10.1103/PhysRevD.88.112006.

[5] CMS Collaboration, "Search for long-lived neutral particles decaying to quark-antiquark pairs in proton-proton collisions at $\sqrt{s} = 8$ TeV", *Phys. Rev. D* **91** (Jan, 2015) 012007, doi:10.1103/PhysRevD.91.012007.

[6] CMS Collaboration, "Search for long-lived neutral particles in the final state of delayed photons and missing energy in proton-proton collisions at $\sqrt{s}$ = 8 TeV", Technical Report CMS-PAS-EXO-12-035, CERN, Geneva, 2015.

[7] CMS Collaboration, "Search for displaced photons using conversions at 8 TeV", Technical Report CMS-PAS-EXO-14-017, CERN, Geneva, 2015.

[8] ATLAS Collaboration, "Search for nonpointing and delayed photons in the diphoton and missing transverse momentum final state in 8 TeV pp collisions at the LHC using the ATLAS detector", *Phys. Rev. D* **90** (Dec, 2014) 112005, doi:10.1103/PhysRevD.90.112005.

[9] CMS Collaboration, "Search for long-lived particles that decay into final states containing two electrons or two muons in proton-proton collisions at $\sqrt{s} = 8$ TeV", *Phys. Rev. D* **91** (Mar, 2015) 052012, doi:10.1103/PhysRevD.91.052012.

[10] CMS Collaboration, "Search for Displaced Supersymmetry in events with an electron and a muon with large impact parameters", *Phys. Rev. Lett.* **114** (2015), no. 6, 061801, doi:10.1103/PhysRevLett.114.061801, arXiv:1409.4789.

[11] ATLAS Collaboration, "Search for massive, long-lived particles using multitrack displaced vertices or displaced lepton pairs in pp collisions at $\sqrt{s} = 8$ TeV with the ATLAS detector", *Phys. Rev. D* **92** (Oct, 2015) 072004, doi:10.1103/PhysRevD.92.072004.

[12] P. Graham, D. Kaplan, S. Rajendran, and P. Sarawat, "Displaced Supersymmetry", *Journal of High Energy Physics* **149** (2012) doi:10.1007/JHEP07(2012)149, arXiv:1204.6038.

[13] T. Sjostrand, S. Mrenna, and P. Z. Skands, "A brief introduction to PYTHIA 8.1", *Comput. Phys. Commun.* **178** (2008) 852–867, doi:10.1016/j.cpc.2008.01.036, arXiv:0710.3820.

[14] J. Alwall et al., "A Standard format for Les Houches event files", *Computer Physics Communications* **176** (2007), no. 4, 300 – 304, doi:10.1016/j.cpc.2006.11.010.

[15] B. Allanach et al., "The Snowmass points and slopes: Benchmarks for SUSY searches", *Eur.Phys.J.* **C25** (2002) 113–123, doi:10.1007/s10052-002-0949-3, arXiv:hep-ph/0202233.

[16] CMS Collaboration, "Particle-Flow Event Reconstruction in CMS and Performance for Jets, Taus, and MET", Technical Report CMS-PAS-PFT-09-001, CERN, Geneva, 2009.

[17] CMS Collaboration, "Performance of CMS muon reconstruction in pp collision events at $\sqrt{s}$=7 TeV", *Journal of Instrumentation* **7** (2012) doi:10.1088/1748-0221/7/10/P10002, arXiv:1206.4071.

[18] CMS Collaboration, "Commissioning of the Particle-Flow reconstruction in Minimum-Bias and Jet Events from pp Collisions at 7 TeV", Technical Report CMS-PAS-PFT-10-002, CERN, Geneva, 2010.

[19] "Performance of electron reconstruction and selection with the CMS detector in proton-proton collisions at sqrt(s) = 8 TeV", *Journal of Instrumentation* **10** (2015), no. 06, P06005.

[20] M. Cacciari and G. P. Salam, "Pileup subtraction using jet areas", *Phys.Lett.* **B659** (2008) 119–126, doi:10.1016/j.physletb.2007.09.077, arXiv:0707.1378.

[21] CMS Collaboration, "Identification of b quark jets at the CMS Experiment in the LHC Run 2", Technical Report CMS-PAS-BTV-15-001, CERN, Geneva, 2016.

[22] M. Kramer et al., "Supersymmetry production cross sections in pp collisions at $\sqrt{s} = 7$ TeV", arXiv:1206.2892.

[23] J. Alwall, P. Schuster, and N. Toro, "Simplified models for a first characterization of new physics at the LHC", *Phys. Rev. D* **79** (2009) 075020, doi:10.1103/PhysRevD.79.075020, arXiv:0810.3921.

[24] CMS Collaboration, "Interpretation of searches for supersymmetry with simplified models", *Phys. Rev. D* **88** (2013) 052017, doi:10.1103/PhysRevD.88.052017, arXiv:1301.2175.